

# Self-monitoring of fatigue damage and dynamic strain in carbon fiber polymer–matrix composite

Xiaojun Wang and D.D.L. Chung\*

Composite Materials Research Laboratory, State University of New York at Buffalo,  
Buffalo, NY 14260-4400, USA

(Received 3 September 1996; accepted 22 May 1997)

Self-monitoring of static/fatigue damage and dynamic strain in a continuous crossply [0/90] carbon fiber polymer–matrix composite by electrical resistance ( $R$ ) measurement was achieved. With a static/cyclic tensile stress along the  $0^\circ$  direction,  $R$  in this direction and  $R$  perpendicular to the fiber layers were measured. Upon static tension to failure,  $R$  in the  $0^\circ$  direction first decreased (due to increase of degree of  $0^\circ$  fiber alignment and fiber residual compressive stress reduction) and then increased (due to  $0^\circ$  fiber breakage), while  $R$  perpendicular to the fiber layers increased monotonically (due to increase of degree of  $0^\circ$  fiber alignment and delamination). Upon cyclic tension,  $R$  ( $0^\circ$ ) decreased reversibly, while  $R$  perpendicular to the fiber layers increased reversibly, though  $R$  in both directions changed irreversibly by a small amount after the first cycle. Upon fatigue testing at a maximum stress of 57% of the fracture stress,  $R$  ( $0^\circ$ ) irreversibly increased both in spurts and continuously, due to  $0^\circ$  fiber breakage, which started at 15% of the fatigue life, while  $R$  (perpendicular to the fiber layers) irreversibly increased both in spurts and continuously, due to delamination, which started at 33% of the fatigue life. The peak  $R$  ( $0^\circ$ ) in a cycle irreversibly decreased, while the minimum  $R$  (perpendicular to the fiber layers) at the end of a cycle irreversibly increased during the first 0.1% of the fatigue life, due to irreversible increase in the degree of  $0^\circ$  fiber alignment.  $R$  ( $0^\circ$ ) became noisy starting at 87% of the fatigue life, whereas  $R$  (perpendicular to the fiber layers) became noisy starting at 50% of the fatigue life. For a [90] unidirectional composite,  $R$  ( $0^\circ$ ) increased reversibly upon tension and decreased reversibly upon compression in the  $0^\circ$  direction, due to piezoresistivity. © 1997 Elsevier Science Ltd. All rights reserved.

(Keywords: composite; carbon fiber; polymer; electrical; resistance; fatigue; strain; monitoring)

## INTRODUCTION

Because of the brittleness of carbon fiber composites, the monitoring of their damage during use is desirable so as to provide remedies or changes in service conditions before catastrophic failure takes place. This monitoring requires sensors, such as strain sensors. These sensors can be placed in strategic locations of the composite structure. They can be optical fibers, piezoelectric sensors, piezoresistive sensors, etc. Structures having this sensing ability are commonly known as smart structures. Although the placement of sensors is common in smart structures, it suffers from poor durability (due to the tendency for the attached sensors to come off from the structure or to be damaged during use of the structure), limited sensing volume (due to the fact that each sensor can only sense the strain in its immediate vicinity and the impracticality of having sensors covering the whole structure), degradation of

mechanical properties (due to the embedding of the sensors between plies of carbon fibers in the composite, the large size of a sensor compared to the diameter of a carbon fiber, and the ineffectiveness of the sensors to serve as a reinforcement), and high cost (due to the high cost of the sensors, and in some cases, of the peripheral equipment, such as lasers and electronics, needed for the sensors to function). Self-monitoring refers to the ability for the structural material to monitor itself; i.e., the structural material is itself a sensor, so that there is no need to place any sensor on the structure. By using a self-monitoring material, the disadvantages mentioned above are removed, as the structural material is durable and the whole structure (not just in limited locations) can sense.

Fatigue occurs in most materials during dynamic loading at stress amplitudes below the fracture strength. Fatigue failure is the cause of numerous disasters, such as those related to aeroplanes, automobiles, ships, bridges and machinery, since dynamic loading is commonly encountered. Fatigue monitoring is conventionally performed by

\* Author to whom correspondence should be addressed.

monitoring at a frequency of at most once a loading cycle (usually once in dozens of cycles) because the monitoring (commonly by acoustic emission) is restricted to the damage only and reversible strain cannot be monitored anyway. Because fatigue monitoring conventionally occurs without dynamic strain monitoring, one cannot determine the loading cycle at which damage occurs unless the loading is periodic in time.

The most commonly used method of fatigue monitoring is acoustic emission<sup>1,2</sup>, which suffers from its inability to monitor dynamic strain. Much less common is the method involving the measurement of the electrical resistance, which increases due to damage and provides a mechanism for self-monitoring. Previous work using electrical resistance to monitor fatigue was carried out on a CaF<sub>2</sub>-matrix SiC-whisker composite<sup>3</sup>, but dynamic strain monitoring was not performed, probably because this composite's electrical resistivity did not change reversibly with reversible strain. In general, dynamic strain monitoring requires a measurand which changes in value reversibly during reversible straining. In addition, in order for both dynamic strain and damage to be simultaneously monitored with a single method, that method must involve a measurand which changes in value reversibly during reversible straining and changes irreversibly during damage. In this work, we have achieved this by using the electrical resistance as the measurand and continuous carbon fiber polymer-matrix composite as the material.

Continuous carbon fiber polymer-matrix composites are advanced composites which are attractive in that they combine high strength, high modulus and low density. Previous work on a polymer-matrix composite containing a combination of continuous glass fibers and continuous carbon fibers has shown that the electrical resistance of this composite increases irreversibly upon damage (due to the fracture of the carbon fibers)<sup>4</sup>, but fatigue monitoring and reversible resistivity changes (dynamic strain monitoring) were not explored. Our previous work on continuous unidirectional (0°) carbon fiber polymer-matrix composite<sup>5,6</sup> has shown that both the longitudinal (parallel to fibers) and transverse (perpendicular to fiber layers) electrical resistivities of the composite change reversibly upon dynamic straining (due to the reversible change in the degree of fiber alignment and fiber residual compressive stress reduction) and change irreversibly upon damage (due to irreversible change in the degree of neatness of the fiber arrangement within a fiber bundle after the first strain cycle). Furthermore, fatigue monitoring simultaneous to dynamic strain monitoring was demonstrated by longitudinal electrical resistance measurement; fiber breakage during fatigue caused the longitudinal resistance to increase irreversibly<sup>6</sup>. This paper extends Refs.<sup>5,6</sup> in that it addresses unidirectional [90] and crossply [0/90] fiber composites, whereas Refs.<sup>5,6</sup> address only unidirectional [0] ones. Furthermore, this paper uses both longitudinal and transverse resistivities for fatigue self-monitoring, whereas Ref.<sup>6</sup> uses only the longitudinal resistivity for this purpose.

**Table 1** Carbon fiber and epoxy matrix properties (according to ICI Fiberite)

10E — Torayca T-300 (6K) untwisted, UC-309 sized	
Diameter	7 $\mu\text{m}$
Density	1.76 $\text{g cm}^{-3}$
Tensile modulus	221 GPa
Tensile strength	3.1 GPa
976 Epoxy	
Process temperature	350°F (177°C)
Maximum service temperature	350°F (177°C) dry 250°F (121°C) wet
Flexural modulus	3.7 GPa
Flexural strength	138 MPa
$T_g$	232°C
Density	1.28 $\text{g cm}^{-3}$

## EXPERIMENTAL METHODS

Composite samples were constructed from individual layers cut from a 12 in wide unidirectional carbon fiber prepreg tape manufactured by ICI Fiberite (Tempe, AZ). The product used was Hy-E 1076E, which consisted of a 976 epoxy matrix and 10E carbon fibers. The fiber and matrix properties are shown in *Table 1*.

The composite laminates were laid up in a 4 × 7 in (102 × 178 mm) platen compression mold with laminate configuration [90]<sub>32</sub> for the unidirectional composite and [0/90]<sub>35</sub> for the crossply composite. The individual 4 × 7 in fiber layers (32 per laminate for the 90° unidirectional composite and 12 per laminate for the crossply composite) were cut from the prepreg tape. The layers were stacked in the mold with a mold release film on the top and bottom of the layup. No liquid mold release was necessary. The density of the laminate was 1.52 ± 0.03 and 1.50 ± 0.03  $\text{g cm}^{-3}$  for 90° unidirectional and crossply composites respectively. The thickness of the laminate was 4.5 and 1.5 mm for the [90] unidirectional and crossply composites respectively. The volume fraction of carbon fibers in the composite was 58% and 52% for the 90° unidirectional and crossply composites respectively. The laminates were cured using a cycle based on the ICI Fiberite C-5 cure cycle. The curing occurred at 179 ± 6°C (355 ± 10°F) and 0.61 MPa (89 psi) for 120 min. Afterwards, they were cut to pieces of size 160 × 14 mm. With 6000 fibers per bundle and 7  $\mu\text{m}$  diameter for a fiber, there were thirteen 0° fiber bundles in a [0/90] specimen for static tensile testing. Glass fiber reinforced epoxy end tabs were applied to both ends on both sides of each piece, such that each tab was 30 mm long and the inner edges of the end tabs on the same side were 100 mm apart. The tensile strength was 62 ± 4.9 and 695 ± 18 MPa for the [90] unidirectional and crossply composites respectively. The tensile ductility was (0.74 ± 0.08)% and (1.06 ± 0.18)% for the [90] unidirectional and crossply composites respectively. The Poisson ratio was 0.05 and 0.013 for the unidirectional and crossply composites, respectively. The electrical resistivity in the 0° direction was 5.74  $\Omega\text{cm}$  and 8.84 × 10<sup>-3</sup>  $\Omega\text{cm}$  for the [90] unidirectional and crossply composites respectively; that in the direction perpendicular to the fiber layers was 6.25

and 4.57  $\Omega\text{cm}$  for unidirectional and crossply composites, respectively.

The electrical resistance  $R$  was measured both in the  $0^\circ$  direction and in the direction perpendicular to the fiber layers using the four-probe method while either static or cyclic tension was applied in the  $0^\circ$  direction. Silver electrically conducting paint was used for all electrical contacts. The four probes consisted of two outer current probes and two inner voltage probes. The resistance  $R$  refers to the sample resistance between the inner probes. For measuring  $R$  in the  $0^\circ$  direction (the stress axis), the four electrical contacts were around the whole perimeter of the sample in four parallel planes that were perpendicular to the stress axis, such that the inner probes were 60 mm apart and the outer probes were 80 mm apart. For measuring  $R$  in the direction perpendicular to the fiber layers, the current contacts were centered on the largest opposite faces parallel to the stress axis and in the form of open rectangles of length 75 mm in the stress direction and width 11 mm, while each of the two voltage contacts was in the form of a solid rectangle (of length 20 mm in the stress direction) surrounded by a current contact (open rectangle). Thus, each face had a current contact surrounding a voltage contact. A strain gage was attached to the center of one of the largest opposite faces parallel to the stress axis for samples for measuring  $R$  in the  $0^\circ$  direction as well as samples for measuring  $R$  in the direction perpendicular to the fiber layers. A Keithley 2001 multimeter was used for d.c. electrical measurement. The displacement rate was 1.0 mm  $\text{min}^{-1}$  for the crossply composite, and was 0.5 mm  $\text{min}^{-1}$  for the [90] unidirectional composite. A hydraulic mechanical testing system (MTS 810) was used for tension-tension cyclic loading in the  $0^\circ$  direction, with stress ratio (minimum stress to maximum stress in a cycle) 0.05 and with maximum stress 395 MPa (at which strain equals 0.57%) for the crossply composite. The secant modulus was determined at the maximum stress in every cycle. Each cycle took 1 s (except 2 s in the case of fatigue monitoring through measurement of the resistance perpendicular to the fiber layers). The total number of cycles before fatigue failure was 211 795 for the crossply composite used to measure  $R$  ( $0^\circ$ ) and was, on the average, 217 392 for the crossply composite used to measure  $R$  perpendicular to the fiber layers. Although the results shown in this paper are for two particular fatigue tests, testing of similar samples confirmed that the results presented here are reproducible.

## RESULTS AND DISCUSSION

### Static loading to failure

Figure 1 shows the tensile stress, strain and  $\Delta R/R_0$  (fractional increase in resistance) along the stress direction, which is the  $0^\circ$  direction, obtained simultaneously during static tensile loading up to failure for the crossply composite. This  $\Delta R/R_0$  first decreased and then increased in steps as the strain increased. Essentially the same

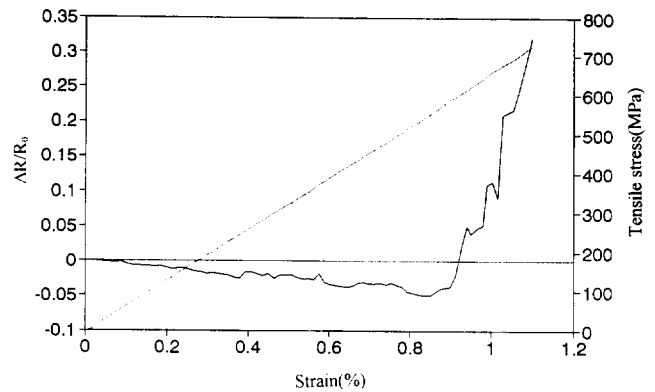


**Figure 1** Tensile stress, strain and  $\Delta R/R_0$  in the  $0^\circ$  direction of crossply composite obtained simultaneously during static tension up to fracture, which occurs at the highest strain in the curves. Solid curve:  $\Delta R/R_0$  vs. strain. Dashed curve: stress vs. strain

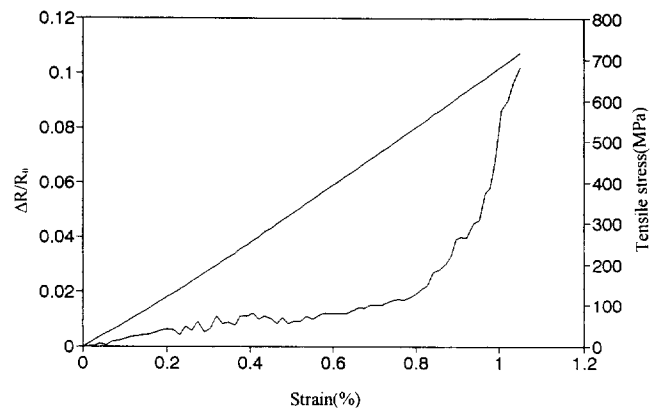


**Figure 2** Tensile stress, strain and  $\Delta R/R_0$  in the direction perpendicular to the fiber layers of crossply composite obtained simultaneously during static tension up to fracture, which occurs at the highest strain in the curves. Solid curve:  $\Delta R/R_0$  vs. strain. Dashed curve: stress vs. strain

behavior was observed for the unidirectional composite of Ref.<sup>5</sup> (Fig. 2 of Ref.<sup>5</sup>).

Figure 2 shows the tensile stress, strain (in the  $0^\circ$  direction) and  $\Delta R/R_0$  along the direction perpendicular to the fiber layers, obtained simultaneously during static loading up to failure for the crossply composite. This  $\Delta R/R_0$  increased gradually with increasing strain and then increased abruptly from  $\Delta R/R_0 = 0.02$  as the strain increased beyond 0.8%, such that  $\Delta R/R_0$  reached a maximum of 0.10. In contrast, for the unidirectional composite of Ref.<sup>5</sup> (Fig. 4 of Ref.<sup>5</sup>), this  $\Delta R/R_0$  increased abruptly with increasing strain at strains below 0.13% and then increased gradually as the strain further increased up to failure, such that  $\Delta R/R_0$  reached a maximum of 0.44.

As explained in Ref.<sup>5,6</sup>, the gradual decrease of  $\Delta R/R_0$  along the stress axis with increasing strain from 0 to 0.85% (Figure 1) is due to the increase in the degree of  $0^\circ$  fiber alignment and to the reduction of the residual compressive stress in the fiber. The abrupt increase in this  $\Delta R/R_0$  at strains beyond 0.85% (Figure 1) is due to  $0^\circ$  fiber breakage. For  $\Delta R/R_0$  in the direction perpendicular to the fiber layers, the abrupt increase of  $\Delta R/R_0$  at strains below 0.13% in the

case of the crossply composite of Ref.<sup>5</sup> is due to the increase in the degree of 0° fiber alignment and the consequent decrease in the chance that adjacent fiber layers touch one another, as explained in Ref.<sup>5</sup>. In the case of the crossply composite, the presence of the 90° fibers, which are perpendicular to the stress axis, makes the increase in the degree of 0° fiber alignment only slightly affect the chance that adjacent fiber layers touch one another. As a result, the abrupt increase in  $\Delta R/R_0$  at strains below 0.13%, as observed in the [0] unidirectional composite, was not observed in the crossply composite and the maximum  $\Delta R/R_0$  is much smaller for the crossply composite than the [0] unidirectional composite. Nevertheless, the slight (up to 0.1 only) but abrupt increase in  $\Delta R/R_0$  with strain beyond 0.85% in Figure 2 is still attributed to the increase in the degree of 0° fiber alignment.

Dynamic loading

Figure 3 shows the tensile stress, strain and  $\Delta R/R_0$  along the stress axis (in the 0° direction) obtained simultaneously for the crossply composite during cyclic tension to a stress amplitude equal to 35% of the breaking stress. The strain returned to zero at the end of each cycle. Because of the small strains involved,  $\Delta R/R_0$  is essentially equal to the fractional increase in resistivity. The  $\Delta R/R_0$  decreased upon loading and increased upon unloading in every cycle, such that  $R$  irreversibly decreased slightly after the first cycle (i.e.,  $\Delta R/R_0$  did not return to 0 at the end of the first cycle). The behavior of Figure 3 is the same as that of the 0° unidirectional composite of Ref.<sup>5</sup> (Fig. 1 of Ref.<sup>5</sup>), except that the magnitude of  $\Delta R/R_0$  is smaller. That the magnitude of  $\Delta R/R_0$  is smaller for the crossply composite than the unidirectional composite at stress amplitudes equal to essentially the same fraction of the corresponding breaking stresses is because the crossply composite has 90° fibers.

A length increase without any resistivity change would have caused  $R$  to increase during tensile loading. In contrast,  $R$  was observed to decrease (not increase) upon tensile loading. Furthermore, for the crossply composite, the observed magnitude of  $\Delta R/R_0$  was about 6 times that of  $\Delta R/R_0$  calculated by assuming that  $\Delta R/R_0$  was only due to length increase and not due to any resistivity change. Hence, the contribution of  $\Delta R/R_0$  from the length increase is negligible compared to that from the resistivity change.

For both [0] unidirectional and crossply composites, the irreversible decrease in  $\Delta R/R_0$  in the 0° direction at the end of the first cycle is due to the irreversible decrease in the degree of waviness of the 0° fibers after the first cycle.

Figure 4 shows the tensile stress, strain (in the 0° direction) and  $\Delta R/R_0$  perpendicular to the fiber layers obtained simultaneously for the crossply composite during cyclic tension to a stress amplitude equal to 35% of the breaking stress. The strain returned to zero at the end of each cycle. The  $\Delta R/R_0$  increased upon loading and decreased upon unloading in every cycle, such that  $R$  irreversibly increased slightly after the first cycle (i.e.,  $\Delta R/R_0$  did not return to 0 at the end of the first cycle). The behavior of Figure 4 is similar to that of the [0] unidirectional composite of Ref.<sup>5</sup> (Fig. 3 of Ref.<sup>5</sup>), except that  $\Delta R/R_0$  is smaller by

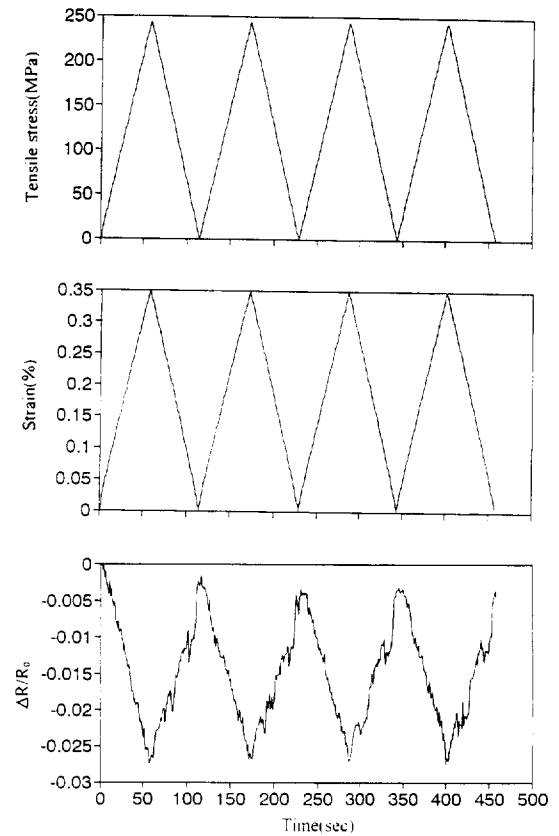


Figure 3 Variation of  $\Delta R/R_0$  (0° direction), tensile stress and tensile strain with cycle number during cyclic tension to a stress amplitude equal to 35% of the fracture stress for crossply composite

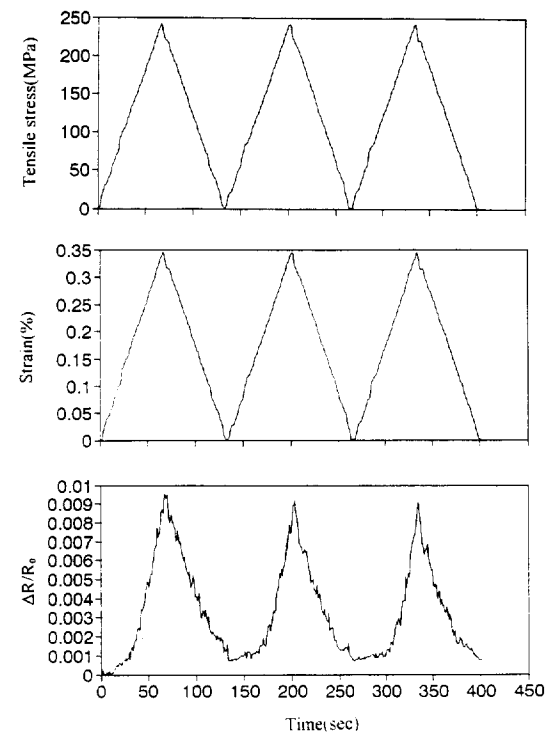


Figure 4 Variation of  $\Delta R/R_0$  (direction perpendicular to the fiber layers), tensile stress and tensile strain with cycle number during cyclic tension to a stress amplitude equal to 35% of the fracture stress for crossply composite

about 85% and the irreversible portion of  $\Delta R/R_0$  is positive for the crossply composite but negative for the 0° unidirectional composite. The small value of  $\Delta R/R_0$  for the crossply composite compared to the unidirectional composite is due to the presence of the 90° fibers in the crossply composite and that these fibers make the increase in the degree of 0° fiber alignment only slightly affect the chance that adjacent fiber layers touch one another. That the irreversible portion of  $\Delta R/R_0$  is negative for the [0] unidirectional composite (Fig. 3 of Ref.<sup>5</sup>) is due to the irreversible decrease in the degree of neatness of the fiber arrangement within a fiber bundle and the consequent increase in the chance that adjacent fiber layers touch one another. That the irreversible portion of  $\Delta R/R_0$  is positive for the crossply composite (Figure 4) is due to the presence of the 90° fibers, which (i) make the irreversible decrease in the degree of neatness of the fiber arrangement have negligible effect on the chance that the adjacent fiber layers touch one another, and (ii) cause the 0° fibers to be somewhat wavy (with the 0° fibers partly penetrating the gap between the 90° fiber bundles of the adjacent 90° fiber layer) after composite fabrication by compression molding and this waviness enhances the chance for the 0° and 90° fiber layers to touch each other. After a cycle of tensile loading in the 0° direction, the waviness is irreversibly lessened, thereby decreasing the chance for the adjacent fiber layers to touch each other and thus irreversibly increasing  $R$  perpendicular to the fiber layers.

Dynamic tensile loading was conducted on crossply composites at different stress amplitudes. The results at a stress amplitude equal to 35% of the fracture stress are shown in Figure 3 for  $\Delta R/R_0$  in the 0° direction and in Figure 4 for  $\Delta R/R_0$  perpendicular to the fiber layers. The behavior at different stress amplitudes are similar, though the magnitudes of both reversible and irreversible portions of  $\Delta R/R_0$  in both directions increase with increasing stress amplitude, as shown in Table 2. Table 2 also shows comparison of  $\Delta R/R_0$  between the crossply composite of this work and the unidirectional composite of Ref.<sup>5</sup>. For the same stress amplitude (expressed as a fraction of the fracture stress), the magnitudes of both reversible and irreversible portions of  $\Delta R/R_0$  in both directions are higher for the unidirectional composite than the crossply composite.

Both dynamic tensile loading and dynamic compressive

**Table 2** Effect of stress amplitude and fiber lay-up configuration on the reversible and irreversible parts of  $\Delta R/R_0$

Maximum stress/ Fracture stress	$\Delta R/R_0$ , parallel to 0° fibers		$\Delta R/R_0$ , perpendicular to the fiber layers	
	Reversible	Irreversible	Reversible	Irreversible
6.1% <sup>a</sup>	-0.0015	0	0.0020	0
9.2% <sup>a</sup>	-0.0057	-0.00043	0.0030	0.00039
19.4% <sup>a</sup>	-0.0122	-0.00287	0.0061	0.00054
35% <sup>a</sup>	-0.0263	-0.00357	0.0090	0.00072
73.6% <sup>a</sup>	-0.0389	-0.00584	/	/
35-36% <sup>b</sup>	-0.0680	-0.01200	0.0600	-0.01700

<sup>a</sup>Crossply composite of this work.

<sup>b</sup>Unidirectional composite of Ref.<sup>5</sup>

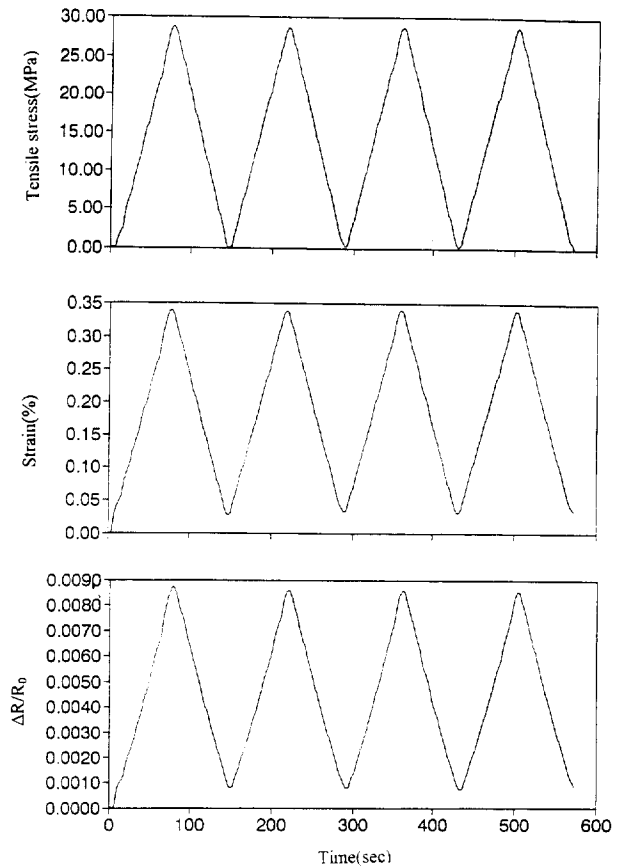


**Figure 5** Tensile stress, strain and  $\Delta R/R_0$ , all in the direction perpendicular to the fibers, in a 90° unidirectional composite

**Table 3** Strain sensitivity (or gage factor) in the 0° direction

Composite type	Maximum stress/ Fracture stress	Strain sensitivity
0° unidirectional	32%	-35.7 <sup>a</sup>
	36%	-37.6 <sup>a</sup>
Crossply	19.4%	-5.7 <sup>a</sup>
	35%	-7.1 <sup>a</sup>
90° unidirectional	/	2.2 <sup>a</sup>
	/	-2.1 <sup>b</sup>

<sup>a</sup>Tension

<sup>b</sup>Compression

loading were conducted on the [90] unidirectional composite, as shown in Figures 5 and 6 respectively. Stress was applied in the 0° direction while the electrical resistance in the 0° direction was measured and the fibers were in the 90° direction. The resistance increased upon tension (Figure 5) and decreased upon compression (Figure 6). The effect was not totally reversible due to plastic deformation, which is attributed to the polymer matrix, as the polymer matrix dominated the mechanical properties perpendicular to the fibers. The reversible resistance changes under tension and compression are due to piezoresistivity, which refers to the phenomenon in which the resistivity of a composite with a conducting filler increases upon increase of the distance between filler units during tension and decreases upon decrease of this distance during compression.

The strain sensitivity or gage factor is defined as the

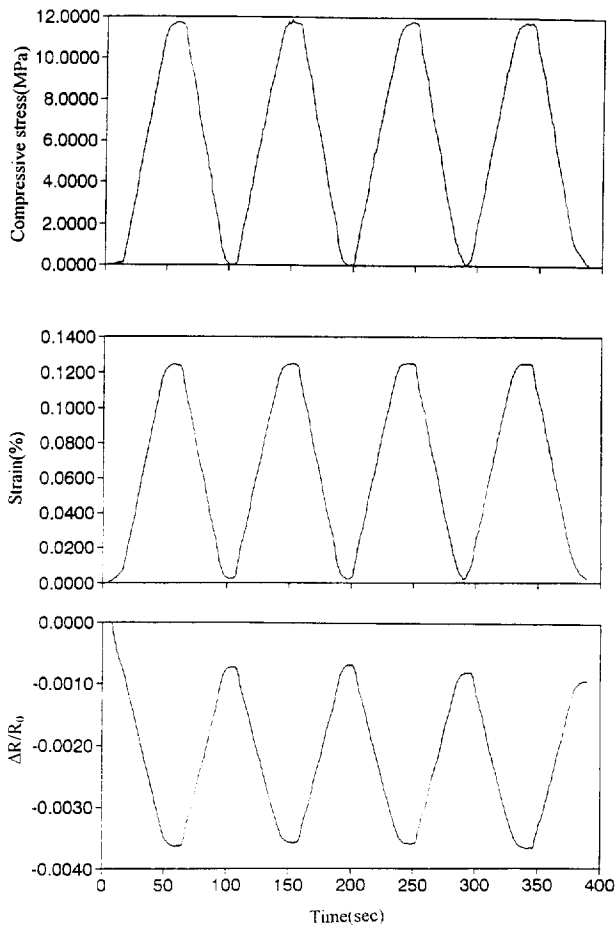


Figure 6 Compressive stress, strain and  $\Delta R/R_0$ , all in the direction perpendicular to the fibers, in a  $90^\circ$  unidirectional composite

reversible part of  $\Delta R/R_0$  divided by the strain amplitude. Its values in the  $0^\circ$  direction are shown in Table 3 for the [0] and [90] unidirectional composites as well as the [0/90] crossply composite. The magnitude of the strain sensitivity is much higher for the  $0^\circ$  unidirectional composite than the crossply composite and is smallest for the [90] unidirectional composite. This means that the contribution of the  $90^\circ$  fibers (i.e., piezoresistivity) to the resistance change observed in the crossply composite is small. The strain sensitivity for the crossply composite is not equal to the average of the values for the [0] and [90] unidirectional composites, due to the interaction between the  $0^\circ$  and  $90^\circ$  fiber layers in the crossply composite.

*Fatigue testing*

*Resistance in the  $0^\circ$  direction.* Figure 7 shows  $\Delta R/R_0$ , tensile stress and tensile strain simultaneously obtained in the  $0^\circ$  direction during cyclic tension–tension loading of the crossply composite. The maximum stress was 395 MPa, or 57% of the fracture stress. The maximum strain was 0.57%. The stress and strain did not return to zero at the end of each cycle, as shown in Figure 8. The resistance  $R$  decreased upon loading and increased upon unloading in every cycle, such that  $R$  irreversibly decreased after the first

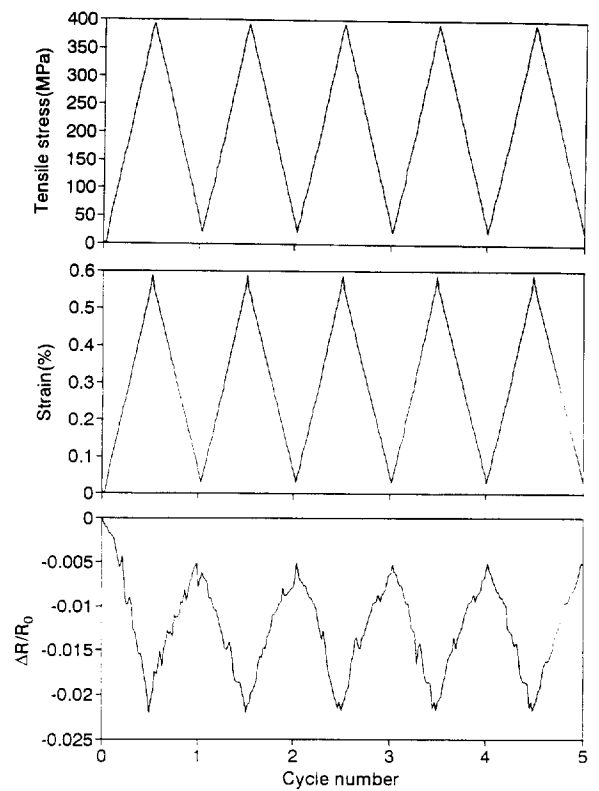


Figure 7 Variation of  $\Delta R/R_0$  ( $0^\circ$  direction), tensile stress and tensile strain with cycle number during the first few cycles of tension–tension fatigue testing of crossply composite

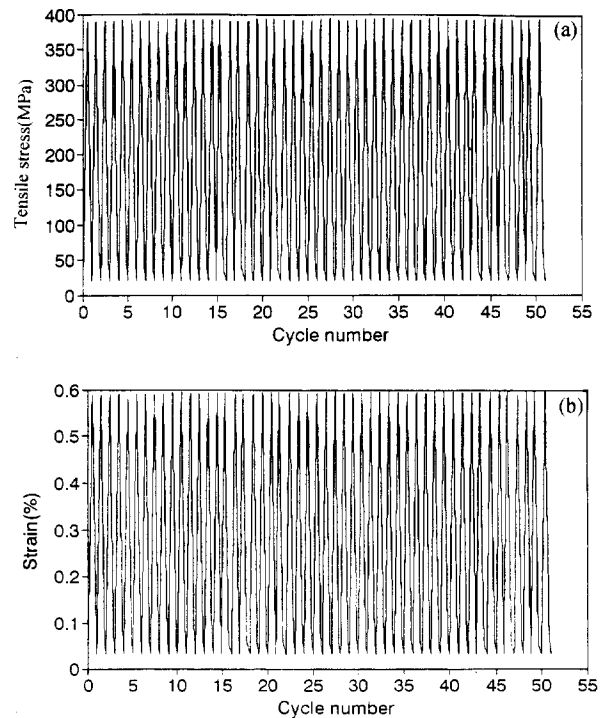
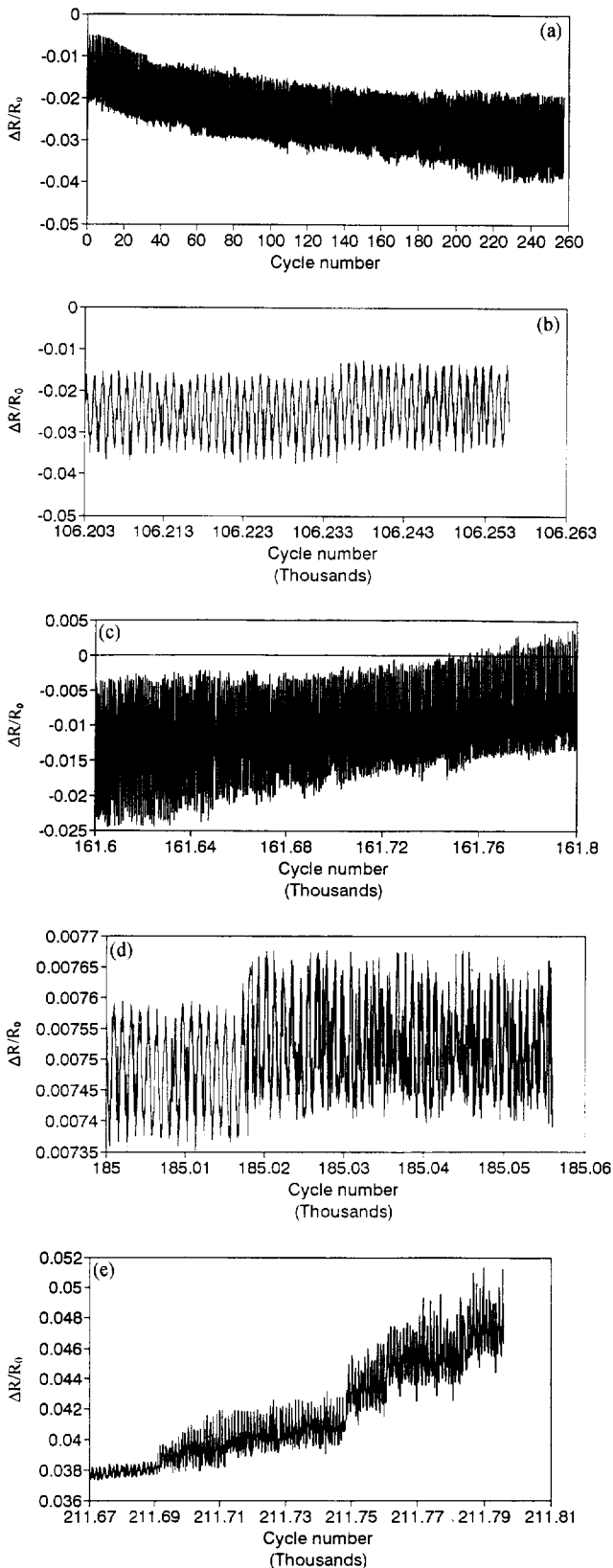
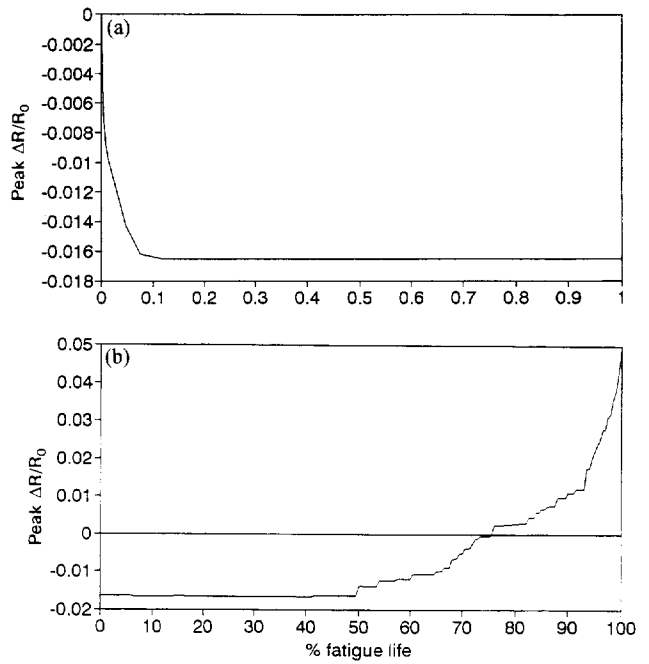


Figure 8 Variation of tensile stress and strain with cycle number during tension–tension fatigue testing of crossply composite



**Figure 9** Variation of  $\Delta R/R_0$  ( $0^\circ$  direction) with cycle number during tension-tension fatigue testing up to failure at 245 975 cycles for crossply composite



**Figure 10** Variation of the peak  $\Delta R/R_0$  ( $0^\circ$  direction) at the end of a cycle with the percentage of fatigue life during tension-tension fatigue testing up to failure for crossply composite

cycle, as in Fig. 1 of Ref.<sup>6</sup> for the  $0^\circ$  unidirectional composite.

During the first 160 cycles (or 0.076% of fatigue life), the peak  $R$  (at the end of the cycle) decreased significantly (*Figure 9(a)* and *Figure 10(a)*). This is attributed to the partially irreversible increase in the degree of  $0^\circ$  fiber alignment at the end of each of the first 160 cycles. This effect is absent in the  $[0]$  unidirectional composite (Fig. 2 of Ref.<sup>6</sup>) due to the presence of the  $90^\circ$  fibers in the crossply composite. The  $90^\circ$  fiber layer was penetrated by the  $0^\circ$  wavy fiber layer after composite fabrication. The extent of penetration decreased slightly after each cycle. At 50% of the fatigue life, spurts of increase started to occur on top of the continuous increase (*Figure 9(b)*). The spurts are due to  $0^\circ$  fiber breakage. The first spurt involved 950 fibers breaking. The spurt at 50% of the fatigue life (at 106,236 cycles) is shown in *Figure 9(b)* and *Figure 10(b)*. As cycling progressed, the peak  $\Delta R/R_0$  continued to increase, such that the peak  $\Delta R/R_0$  increased from values below zero to values above zero (*Figure 9(c)*, (d)). At 87% of the fatigue life (at 185,018 cycles), noise in the  $\Delta R/R_0$  data started to be substantial, as shown by the dark features in *Figure 9(d)* and (e). This noise is attributed to statistical changes in the distance between adjacent  $0^\circ$  and  $90^\circ$  fiber layers, as made possible by significant damage of the polymer matrix. This noise was considerably less in the case of the  $[0]$  unidirectional composite. At 99.95% of the fatigue life (at 211 692 cycles), the peak  $\Delta R/R_0$  started to increase rapidly (*Figure 9(e)*) due to extensive  $0^\circ$  fiber breakage. The rapid increase persisted until fracture at 211 795 cycles.

*Figure 11* shows the fraction of  $0^\circ$  fibers broken during the whole fatigue life, as calculated from *Figure 10* using the method described in Ref.<sup>6</sup>. Fiber breakage started at

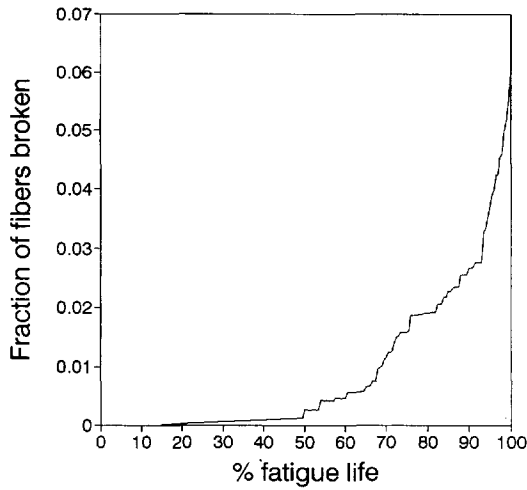


**Figure 11** Variation of the fraction of 0° fibers broken with the percentage of fatigue life during tension–tension fatigue testing up to failure for crossply composite

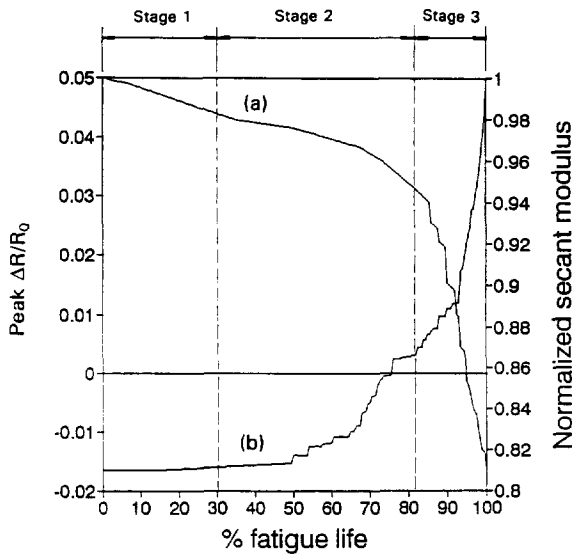


**Figure 12** (a) Normalized secant modulus and (b) peak  $\Delta R/R_0$  at the end of a cycle during tension–tension fatigue testing up to failure for crossply composite

15% of the fatigue life, though it was insignificant until 50% of the fatigue life. Immediate failure occurred when 6% of the fibers were broken.

Comparison of *Figure 11* of this work and Fig. 4 of Ref.<sup>6</sup> shows that fiber breakage started to occur at a smaller fraction of the fatigue life for crossply composite than [0] unidirectional composite.

The normalized secant modulus of the crossply composite is shown versus fatigue life in *Figure 12*. The stiffness decreased from the beginning of fatigue testing. As fatigue continued beyond 70% of fatigue life, the stiffness reduced abruptly. According to the change in peak  $\Delta R/R_0$  and modulus (*Figure 12*), the fatigue life can be divided into three stages, which are attributed to different damage mechanisms. The first stage ranged from the beginning to

30% of fatigue life. The second stage is from 30% to 82% of fatigue life. The third stage is from 82% of fatigue life to failure.

The first stage, from the beginning to 30% of fatigue life, was characterized by decrease in stiffness and a slight increase in peak  $\Delta R/R_0$  at the end of a cycle. Matrix cracking in 90° plies<sup>7</sup> was probably responsible for the behavior in the first stage because matrix cracking initiated in 90° plies which experienced tensile stress in the 0° direction. Since the 0° conductivity of crossply composite is determined by the 0° fibers, the matrix cracks in 90° plies have little effect on the 0° resistance of the composite compared to the effect on the stiffness. The small amount of resistance increase in the first stage suggests that fiber fracture and other damage were relatively minor<sup>8</sup>.

The second stage occurred from 30% to 82% of fatigue life. In this stage, the peak  $\Delta R/R_0$  at the end of a cycle increased in spurts and continuously, and the stiffness kept decreasing. These observations can be explained by the following damage mechanisms. When a crossply composite is loaded in 0° tension, the 0° fibers carry most of the load. The matrix cracks in 90° plies are formed since the 90° plies are weaker than 0° plies when the 0° loading is applied. A contraction within the 0° plies occurs with 0° loading because of the Poisson effect. This contraction is hindered by the 90° plies, which have a higher elastic modulus than in the 0° plies in the 90° direction. In the 0° plies, tensile stresses therefore develop perpendicular to the fiber direction. This can lead to longitudinal (0°) cracks, which tend to initiate at the matrix cracks in the 90° plies. The consequence is fiber fracture, which is indicated by the rapid resistance increase in the second stage. As fatigue progresses, local delamination develops in the interior at intersections of longitudinal and transverse cracks<sup>9</sup>. However, the delamination does not influence the longitudinal resistance significantly. The effect of the delamination on the transverse resistance is significant, which will be discussed in the next section. The matrix cracks, longitudinal cracks, fiber failure and delamination which develop in the second stage have profound effects on the resistance and modulus.

The last stage near the end of fatigue life is characterized by the sharp increase in the peak  $\Delta R/R_0$  and sharp reduction in stiffness as a result of an increase in damage growth rates due to delamination coalescence and further fiber fracture<sup>10</sup>.

*Resistance perpendicular to the fiber layers.* *Figure 13* shows  $\Delta R/R_0$  perpendicular to the fiber layers (i.e., through the thickness), 0° tensile stress and 0° tensile strain simultaneously obtained during cyclic tension–tension loading of the crossply composite. The loading conditions were the same as those for the case of the resistance in the 0° direction. The resistance  $R$  perpendicular to the fiber layers increased upon loading and decreased upon unloading in every cycle, as in *Figure 4*.

During the first 210 cycles (or 0.099% of fatigue life), the minimum  $R$  (at the end of a cycle) as well as the peak  $R$  (in the middle of a cycle) increased gradually cycle after cycle



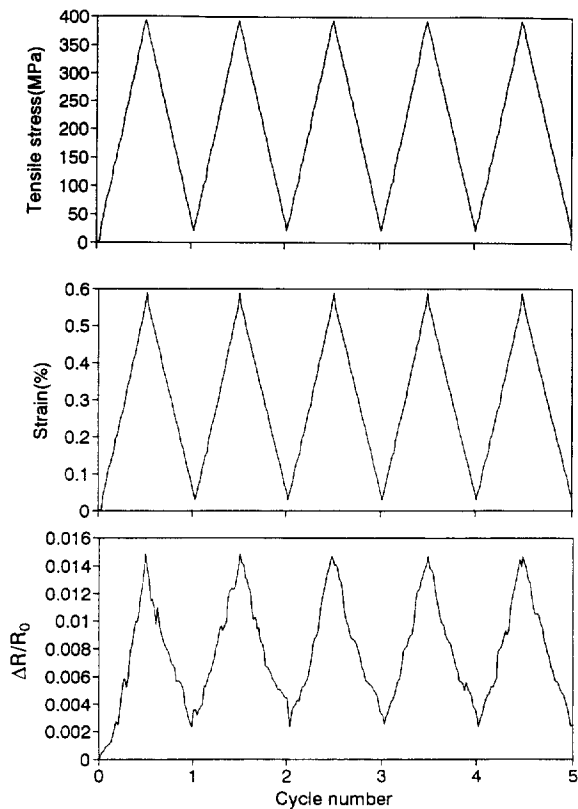


**Figure 13** Variation of  $\Delta R/R_0$  (perpendicular to the fiber layers),  $0^\circ$  tensile stress and  $0^\circ$  tensile strain with cycle number during the first few cycles of tension-tension fatigue testing of crossply composite

(Figure 14(a)). This is attributed partly to the partially irreversible increase in the degree of  $0^\circ$  fiber alignment and partly to matrix cracks, as both tend to decrease the number of contacts between fibers of different layers at the end of each of the first 210 cycles. This effect accompanied the decrease in peak  $R$  ( $0^\circ$ ) at the end of a cycle which was observed during the first 160 cycles (Figure 9(a)). The decrease in peak  $R$  ( $0^\circ$ ) at the end of a cycle was much more significant than the increase in minimum  $R$  (perpendicular to the fiber layers) at the end of a cycle.

After the first 210 cycles, both minimum  $R$  and peak  $R$  (perpendicular to the fiber layers) increased very slowly due to the matrix cracks in  $90^\circ$  plies. These matrix cracks could change the current path perpendicular to the fiber layers and increase the resistance. The first spurt of peak  $R$  (in the middle of a cycle) was observed at 69 987 cycles (33% of fatigue life) (Figure 14(c), (d) and Figure 15). The jump in peak  $R$  is probably due to the  $0^\circ$  cracks and  $0^\circ$  fiber fracture, which change the current path when the composite is loaded in the  $0^\circ$  direction. In Figure 14(c), the minimum  $R$  at the end of a cycle continuously increased while the peak  $R$  in the middle of a cycle showed a jump at 69,987 cycles (33% of fatigue life), after which the peak  $R$  continuously increased in every cycle within Figure 14(c). Subsequently, both minimum  $R$  and peak  $R$  continued to increase in every cycle (Figure 14(e)), but much more gradually than in Figure 14(c). When the composite is unloaded, it is possible that some of the broken fibers will touch each other.

Therefore, the minimum  $R$  (at the end of a cycle) did not show a similar jump as the peak  $R$ . However, the  $0^\circ$  cracks and fiber fracture decreased the chance of fiber contacts so that the minimum  $R$  continuously increased.

As the fatigue testing developed, both minimum  $R$  and peak  $R$  continued to increase in each cycle, as shown in Figure 14(e), but much more gradually than in Figure 14(c). These observations in Figure 14(e) imply that further  $0^\circ$  cracks occurred. Figure 14(f) and Figure 15 show a second resistance spurt at 105 981 cycles (50% of fatigue life). At this spurt, both minimum  $R$  and peak  $R$  jumped together. This is attributed to the formation of local delaminations. The local delamination may be formed around the intersection of the transverse cracks and the  $0^\circ$  cracks. Delamination is expected to greatly affect the resistance through the thickness because the delamination decreases the chance of fibers of adjacent layers to touch each other.

As the fatigue loading continued, more severe resistance changes were observed. At about 62% of fatigue life (Figure 14(g) and Figure 15), the minimum  $R$  (at the end of a cycle) showed a big jump while the peak  $R$  (in the middle of a cycle) increased only gradually, so that the amplitude of the resistance change greatly diminished. The minimum  $R$  showed a big jump because of the irreversible nature of delamination, which was extensive, because local delaminations grew and coalesced. Figure 16 shows the percentage of composite area that exhibited delamination, as calculated from the increase in peak  $\Delta R/R_0$ , assuming that a delaminated area was open-circuited in the direction perpendicular to the fiber layers. Delamination started at 33% of fatigue life and occurred both in spurts and continuously. At 62% of fatigue life, delamination occurred extensively, so that the percent of area delaminated reached 4.3%.

$R$  was observed to be increasingly noisy as the fatigue testing continued (Figure 14(h)). The noisiness was much more than in the case of longitudinal resistance (Figure 9(d) and (e)). Beyond 68% of fatigue life, the noise in  $R$  perpendicular to the fiber layers was so severe that the  $R$  data collection was stopped. As fatigue testing progressed, more delamination and fiber fracture occurred, which made the fiber contacts between adjacent layers more variable and the resistance change therefore became more noisy.

Since the resistance perpendicular to fiber layers is sensitive to the contacting situations between the layers, the measurement of resistance perpendicular to fiber layers can be taken as an indicator of the delamination damage in composites.

## CONCLUSION

Real-time monitoring of static/fatigue damage and dynamic strain in a continuous crossply [0/90] carbon fiber polymer-matrix composite by electrical resistance ( $R$ ) measurement was demonstrated. With a static/cyclic tensile stress along the  $0^\circ$  direction,  $R$  in this direction and  $R$  perpendicular to the fiber layers were measured.

Upon static tension to failure of the [0/90] crossply

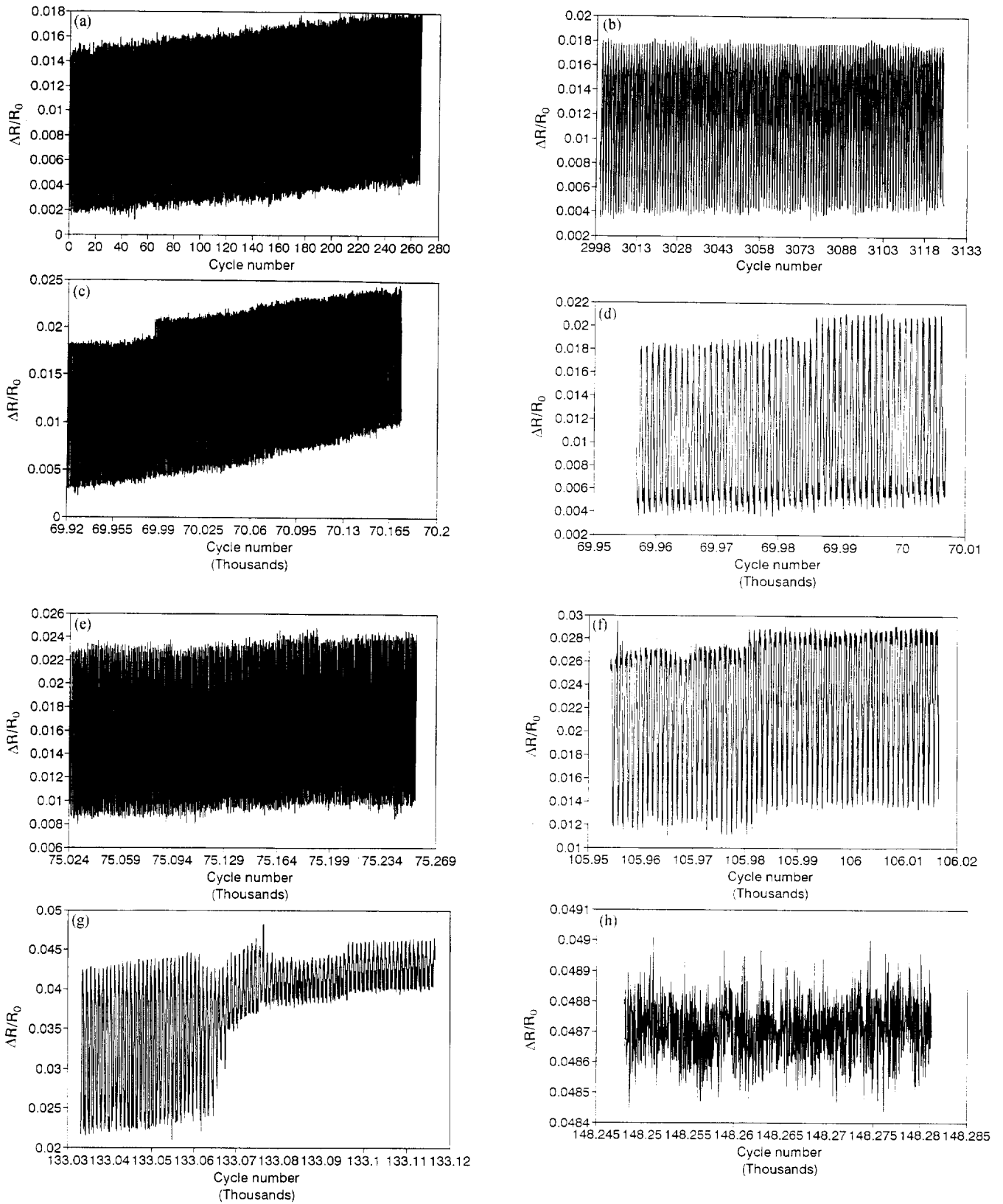


**Figure 14** Variation of  $\Delta R/R_0$  (perpendicular to the fiber layers) with cycle number during tension–tension fatigue testing for crossply composite

composite,  $R$  in the  $0^\circ$  direction first decreased and then increased, while  $R$  perpendicular to the fiber layers increased monotonically. Both the initial decrease of  $R$  in the  $0^\circ$  direction and the increase of  $R$  perpendicular to the

fiber layers are due to the increase of the degree of fiber alignment upon tension, although fiber residual compressive stress reduction upon tension contributes to the former effect<sup>6</sup>. The latter effect was much larger for  $0^\circ$  unidirectional

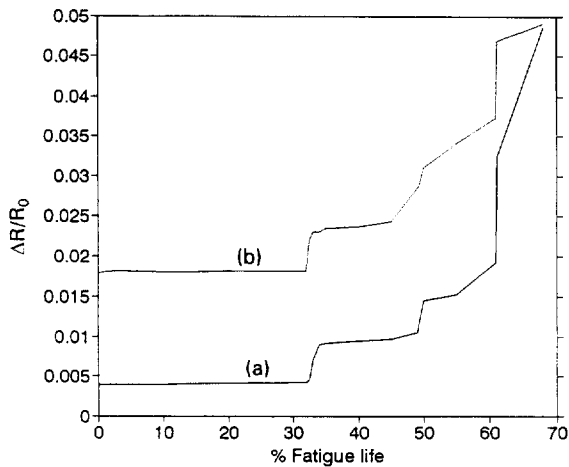


**Figure 15** Variation of  $\Delta R/R_0$  (perpendicular to the fiber layers) with the percentage of fatigue life during tension-tension fatigue for crossply composite. (a) Minimum  $\Delta R/R_0$  at the end of a cycle. (b) Peak  $\Delta R/R_0$  in the middle of a cycle

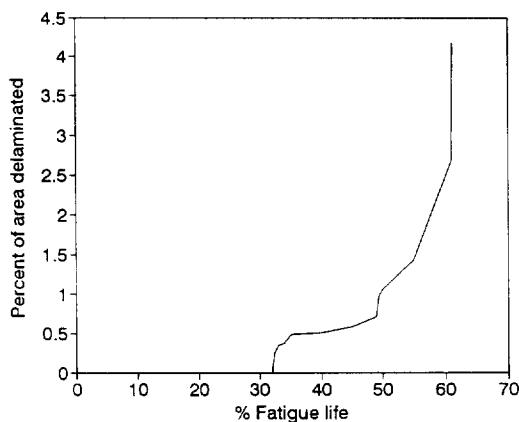


**Figure 16** Variation of the percentage of area delaminated with the percentage of fatigue life during tension-tension fatigue testing for crossply composite

than crossply composites, since the  $90^\circ$  fibers decreased the effect of increasing the degree of fiber alignment on the chance of adjacent fiber layers to touch one another. The later increase of  $R$  in the  $0^\circ$  direction is due to  $0^\circ$  fiber breakage.

Upon cyclic tension of the [0/90] crossply composite,  $R$  in the  $0^\circ$  direction decreased reversibly, while  $R$  perpendicular to the fiber layers increased reversibly, though  $R$  changed irreversibly by a small amount after the first cycle in both directions. The irreversible change was a decrease for  $R$  in the  $0^\circ$  direction for both [0] unidirectional and crossply composites due to the irreversible decrease in the degree of waviness of the  $0^\circ$  fibers. For  $R$  perpendicular to the fiber layers, the irreversible change was a decrease in the case of

the  $0^\circ$  unidirectional composite and an increase in the case of the crossply composite.

For the [90] unidirectional composite,  $R$  in the  $0^\circ$  direction increased reversibly upon tension and decreased reversibly upon compression. Both effects are due to piezoresistivity.

Upon fatigue testing of the [0/90] crossply composite at a maximum stress of 57% of the fracture stress,  $R$  ( $0^\circ$  direction) irreversibly increased both in spurts and continuously, due to fiber breakage, which started at 15% of the fatigue life for the crossply composite, while  $R$  (perpendicular to the fiber layers) irreversibly increased both in spurts and continuously, due to delamination, which started at 33% of the fatigue life. The peak  $R$  ( $0^\circ$ ) at the end of a cycle irreversibly decreased, while the minimum  $R$  (perpendicular to the fiber layers) at the end of a cycle irreversibly increased during the first 0.1% of the fatigue life, due to irreversible increase in the degree of  $0^\circ$  fiber alignment. Moreover,  $R$  ( $0^\circ$ ) became noisy starting at 87% of the fatigue life, whereas  $R$  (perpendicular to the fiber layers) became noisy starting at 62% of the fatigue life. The noise, spurts and continuous  $R$  changes provide progressive indications of the remaining fatigue lifetime.

#### ACKNOWLEDGEMENTS

This work was supported in part by the Center for Electronic and Electro-Optic Materials of the State University of New York at Buffalo.

#### REFERENCES

1. Kozsztowicz, K.J. and Fontaine, D., *J. Am. Ceramic Soc.*, 1990, **73**(10), 2809–2814.
2. Santos-Leal, E. and Lopez, R.J., *Measurement Science & Technology*, 1995, **6**(2), 188–195.
3. Ishida, A., Miyayama, M. and Yanagida, H., *J. Am. Ceram. Soc.*, 1994, **77**(4), 1057–1061.
4. Muto, N., Yanagida, H., Miyayama, M., Nakatsuji, T., Sugita, M. and Ohtsuka, Y., *J. Ceramic Soc. Japan*, 1992, **100**(4), 585–588.
5. Wang, X. and Chung, D.D.L., *Smart Mater. Struct.* 1996, **5**, 796–800.
6. Wang, X. and Chung, D.D.L., *Smart Mater. Struct.*, 1997, **6**, 504–508.
7. Highsmith, L. and Jamison, R.D., in *Composite materials: fatigue and fracture*. ASTM STP-907. ed. H.T. Hahn, Philadelphia, PA, 1986. pp. 233–251.
8. Jamison, D. and Schulte, K., *Characterization and analysis of damage mechanisms in tension-tension fatigue of graphite/epoxy laminates*. ASTM STP-836, 1984. pp. 21–55.
9. Freeman, M., *Characterization of lamina and interlaminar damage in graphite/epoxy composites by deply technique*. ASTM STP-787, 1982. pp. 50–62.
10. O'Brien, K., *Characterization of delamination onset and growth in a composite*. ASTM STP-876, 1985. pp. 282–297.